BNL-211239-2019-JAAM

Energetics and Escape of Interchain-Delocalized Ion Pairs in Nonpolar Media

J. H. Burke, M. J. Bird

To be published in "Advanced Materials"

January 2019

Chemistry Department

Brookhaven National Laboratory

U.S. Department of Energy

USDOE Office of Science (SC), Basic Energy Sciences (BES) (SC-22)

DISCLAIMER

Energetics and Escape of Interchain-Delocalized Ion Pairs in Nonpolar Media

John H. Burke[1], and Matthew J. Bird[2]*

J. H. Burke
Department of Chemistry
University of Vermont
Burlington, VT 05405, United States

Dr. M. J. Bird
Chemistry Division
Brookhaven National Laboratory
Upton, NY 11973, United States
E-mail: mbird@bnl.gov

Keywords: microwave conductivity, charge separation, conjugated polymers, delocalization, ion pair

The electron acceptor F_4TCNQ p-dopes aggregates "nanowires" of poly(3-hexylthiophene) (P3HT) in nonpolar solvents but does not dope unaggregated chains. The standard free energy change for the charge transfer to form an ion pair is ΔG°_{et} = -0.21 eV. The dissociation constant to produce free ions in toluene by DC conductivity is $K^\circ_d = 1 \times 10^{-8} \pm 50\%$ ($\Delta G^\circ_d = 0.48 \pm 0.05$ eV). This remarkably large K°_d, for ions in such a low polarity medium, may reflect interchain delocalization of the hole. The particular characteristics of this material system enable determination of both ΔG°_{et} and ΔG°_d, to find the overall free energy change from the two neutral species to completely separated ions in nonpolar media. It is *endergonic* by +0.27 ± 0.05 eV in contrast to -0.6 eV estimated from reported HOMO LUMO differences, illustrating the challenges that persist in determining such energetics. Steady state microwave conductivity experiments on doped aggregates confirm that holes in the aggregates cannot easily escape their dopant counterion, but at higher dopant concentrations, holes become mobile. These results provide insight into the mechanisms of charge separation involving intermolecularly delocalized charges in nonpolar media, an integral process in organic photovoltaic devices and doped molecular films.

The ability of opposite charges to escape their mutual coulombic attraction in molecular films has long been a puzzle in the field of organic electronics. In media with dielectric constants of $\varepsilon_r = 2 - 3$, point charges, even initially separated by a generous 10 Å, would be bound with energies of 0.72 – 0.48 eV respectively, which is many times the thermal energy available at room temperature (k_BT = 0.026 eV). In non-polar solutions, ion concentrations would have to drop to < pM – nM for entropy to start favoring free ions over ion pairs.

Yet, in both organic photovoltaics (OPVs) and chemically doped conjugated polymer films, charges *do* escape, as evidenced by efficient OPVs[1] and highly conductive doped films.[2] There are many theories to explain this escape, although a common aspect in both cases is the delocalized nature of charges in these highly conjugated materials.[3] In OPVs, charge escape may be assisted by ultrafast photoinduced long-range charge separation,[4] the finite lifetime of interfacial "CT states",[5] energetic disorder,[6] entropic effects unique to bulk heterojunction films,[7] and energy cascades.[8] For the doping of conjugated polymer films with strong electron accepting small molecules, conductivity does not follow simple solution–based ion pairing models.[9] Models for conductivity in doped films have considered the interplay of disorder, state filling, and the overlap of ionized dopant coulomb wells at high dopant concentrations.[10]

There are a number of experimental techniques that can distinguish free charges from paired ones[11] with DC conductivity being one of the better known. Another technique is time resolved microwave conductivity (TRMC).[12] TRMC is a powerful contactless method to selectively probe for the motion of transient *free* charge populations in non-polar media such as the motion of charges along conjugated polymer chains created by flash photolysis (FP-TRMC)[13] or pulse radiolysis (PR-TRMC).[14] The absorption of microwaves tracks the population of non-equilibrium free ions as they are created and ultimately recombine.[15]

We were intrigued by a report from Liu[16] where *steady state* microwave conductivity measurements were used to study the mobility of holes generated by chemical oxidation of

P3HT with $NOSbF_6$ in benzene. Analysis of the data gave a charge mobility, 0.03 cm^2/Vs which was close to, and in fact larger than, the value of 0.014 cm^2/Vs, measured for free holes on P3HT using traditional TRMC techniques.[17] The concentration of ions in their experiment ranged from 6×10^{-7} – 1.8×10^{-5} M. The remarkable unstated implications of measuring a similar mobility with chemical doping in benzene is that either: a) ~100% of ions had escaped their counterion in this non-polar media ($\varepsilon_r = 2.28$), b) that ion-paired holes on P3HT exhibit the same mobility as free holes, or c) a small concentration of free holes have incredibly large mobilities, not previously reported for P3HT. For a simple ion pairing equilibrium model, to have free ions at micromolar concentrations requires a dissociation constant $\geq 10^{-6}$, on the molar scale. For context, we can imagine predicting the dissociation constant for weakly coordinating electrolytes in benzene. LeSuer reported K_d as high as 1.62×10^{-4} for tetrabutylammonium tetrakis(penta-fluorophenyl)borate (TBATFAB) in THF.[18] Given that the free energy for dissociation, ΔG°_d, should be inversely proportional to the dielectric constant, and with $K_d = exp(-\Delta G^{\circ}_d/RT)$ we can estimate that TBATFAB would have K_d ~10^{-13} in benzene.

While not explicitly stated in their paper, evidence presented Figure S1 in SI suggests that regio-regular (RR) P3HT rather than regio-random (RRa) was used by Liu. Unlike RRa-P3HT, RR-P3HT is known to form soluble aggregates in solution through π-π stacking interactions. This process can be controlled to form polycrystalline nanowires (nw-P3HT) of extremely high aspect ratios, with lengths of several microns.[19] These nanowires have significantly different properties to the single chains, exhibiting a bathochromic shift and resolved vibronic structure in the π-π* transition in the UV/vis absorption spectrum.[19-20] This aggregation lowers the oxidation potential of the polymer, allowing for increased reactivity with dopants.[21] Doping induces aggregation in P3HT both kinetically and thermodynamically, through increased planarity of the polymer cation, and increased hole delocalization, respectively.[22] We seek to understand if P3HT aggregates enable unprecedented ion pair dissociation constants in non-polar media.

In this contribution we study ground state chemical doping of nw-P3HT with F_4TCNQ in non-polar solvents with a combination of absorption spectroscopy, microwave conductivity, and DC conductivity. We find that the doping of nw-P3HT by F4TCNQ to make the ion pair (nw-$P3HT^{+\bullet}$,$F_4TCNQ^{-\bullet}$) is energetically marginal *in non-polar media* and establish the free energy change for the process. We test the hypothesis, inspired by Liu's result, that delocalized holes on nw-P3HT might facilitate a remarkable reduction in coulomb binding energy with counterions. We present evidence that supports an unexpectedly large dissociation constant between nw-P3HT holes and $F_4TCNQ^{-\bullet}$ in benzene, but not large enough for most ions to be free at micromolar concentrations to explain Liu's observations. We further confirm that holes on conjugated polymers *do not show microwave conductivity when paired with a counterion*, but like in films, we see evidence of charges, in the aggregates, escaping counterions at very high doping concentrations; this effect is reduced if we try to intercalate the F_4TCNQ into the nw-P3HT. Finally, we combine the equilibrium constants we determined for electron transfer and ion pair dissociation to estimate the free energy change to make separated nw-$P3HT^{+\bullet}$ and $F4TCNQ^{-\bullet}$ ions from their neutral states. We highlight the need for improved methods for determining ion energetics in molecular films given large disparities between our findings and reported HOMO LUMO levels for these materials.

Figure 1a. shows the absorption spectrum of a RR-P3HT solution in toluene containing nanowires and the same solution after heating to 80 $^{\circ}$C to solubilize the chains completely. Data like these were used to establish concentrations of the nanowires in solution by fitting spectra to a linear combination of the solubilized P3HT spectrum, with a known extinction coefficient, and a function containing four gaussians whose integral was determined and kept constant throughout, but whose relative peak heights were allowed to change (see SI for description). This method enabled us to make reasonable estimates of the nanowire concentration in different samples where 0-0 to 0-1 peak ratios varied due to varying H- or J-aggregate character,[19b, 20] causing the extinction coefficient to vary.

Figure 1b. shows that while the addition of F_4TCNQ (0.03 mM) to solutions of nw-P3HT immediately led to absorptions known to be that of P3HT cations and F_4TCNQ anions, there was no such absorption when F_4TCNQ was added to solubilized chains (s-P3HT), even at a higher concentration of 0.13 mM. Doping occurs on longer timescales,[22a] but initial or partial aggregate formation seems to be the rate limiting step. Further evidence for the lack of doping of single chains is provided in Supporting Information. These findings are supported by recent studies of low molecular weight P3HT that does not readily aggregate, where charge transfer with F_4TCNQ in toluene only occurs upon addition of a nonsolvent, decane, which induces aggregation in the polymer.[23] These findings can be explained by the observation that the oxidation potential of P3HT is lowered upon aggregation.[21] Therefore, by doping RR-P3HT with F_4TCNQ in toluene as shown below, we are selectively doping only nw-P3HT.

As F_4TCNQ has been shown to undergo charge transfer with both RRa-P3HT and solvated RR-P3HT in more polar solvents such as chlorobenzene,[21a] this finding highlights the role of solvation energy in stabilization of charge transfer products. Care must be placed when using HOMO and LUMO levels relative to vacuum for molecular films[24] to predict[21a, 23, 25] the driving force of charge transfer in solution: these values appear to show that electron transfer from s-P3HT HOMO to F_4TCNQ LUMO is exoergic by 0.3 eV. The fact that ions are formed adjacently would be expected to make these values even more exoergic by ~ 0.5 eV due to the coulombic attraction and yet no such reaction takes place.

Figure 1c shows the typical evolution of a spectrum containing nw-P3HT as F_4TCNQ is added. A bleach of the neutral nw-P3HT absorption is observed in the region of 600 – 450 nm. The growth at 2100 nm is the P_1 polaron band of P3HT, and the feature from 1100 – 600 nm contains contribution from the P_2 polaron band of the polymer, and the F_4TCNQ anion. A growth is observed at 400 nm, which contains contributions from the F_4TCNQ neutral and anion.

We sought to make an independent estimate of the extinction coefficient of these ions as values found in the literature ranged from 31,000 $M^{-1}cm^{-1}$ at 770 nm[22a] to 85,000 $M^{-1}cm^{-1}$

at 816 nm.[26] However, it was noticed that our estimates of extinction coefficient varied substantially with the concentration of nw-P3HT, indicating an equilibrium. We describe this equilibrium for electron transfer with the following expression for the equilibrium constant, K_{et}:

$$K_{et} = \frac{[ion\ pairs]}{[\mathrm{nwP3HT}_{PRU}][\mathrm{F_4TCNQ}]} = \frac{c_{ip}}{\left([\mathrm{nwP3HT}_{PRU}]_0 - L_p c_{ip}\right)\left([\mathrm{F_4TCNQ}]_0 - c_{ip}\right)} \quad (1)$$

where c_{ip} is the concentration of ion pairs. Polymer repeat unit (PRU) concentration is used to give the concentration of sites that could be doped, with these sites being consumed by polarons, at a rate of L_p sites per polaron, where L_p could represent polaron length or simply number of repeat units consumed upon oxidation. A global fit to the data in Figure 1c and three others, shown in Figure 1d, was performed, using the quadratic solution to the above equilibrium.

The global fitting gave a polaron length of 8.41 ± 0.19 PRU and an equilibrium constant of 3750 ± 200 (ΔG°_{et} = -211 ± 1 meV). This equilibrium constant is of similar magnitude, but smaller than the value of 8000 determined by a Langmuir isotherm model by Moulé and coworkers[27] for P3HT films sequentially doped by F_4TCNQ from an orthogonal solvent.

With optical methods established to determine both aggregate and ion concentrations, steady state microwave conductivity measurements were performed. Solutions of nw-P3HT at 0.136 mM (PRU) were doped with various concentrations of F_4TCNQ, up to a ratio of 40.5 mol% relative to nw-P3HT repeat unit concentration, in toluene. The results are shown in the plots of reflected-to-incident microwave power versus frequency in **Figure 2a**. A minimum in $P_{reflected}$ / $P_{incident}$ is observed at the resonance frequency, as microwave power is transferred to the TE_{102} cavity mode rather than being reflected toward the detector. Changes in the resonance frequency, and changes in $P_{reflected}$ / $P_{incident}$ at the minimum, can be related to changes in the dielectric constant and conductivity, σ, of the sample cavity, respectively.

A model based on transmission line theory[28] was used to fit the data to extract the change in conductivity and change in dielectric constant upon doping. Fitting parameters related

to the instrument, such as cavity dimensions and waveguide impedance, are determined by fitting the data for the empty cavity. For toluene, we found the cavity to be in the overcoupled regime with a quality factor of 53. The sensitivity factor that we obtained from our model was in excellent agreement with that predicted for our cavity using a formula derived by the Delft group[29] giving $\Delta P/P = 120\,\Delta\sigma$ (in S.I. units). We note that using the Delft formula is valid for small (few %) changes in conductivity and would not be appropriate for use if the cavity is close to critically coupled.[16] For the nw-P3HT solutions, all parameters are held constant, save for the conductivity and dielectric constant.

A plot of conductivity versus hole concentration is shown in Figure 2b. At low doping levels, no change in conductivity with increasing hole concentration is observed, which indicates a hole mobility too small to measure. We hypothesize that this is due to the P3HT hole being paired with F_4TCNQ counterions. Optical absorption at 851 nm, shown in Figure S6, taken before and after the microwave conductivity measurement confirmed that the concentration of ions in solutions remained constant throughout with no further ion formation or loss. For hole concentrations above a threshold of ~5 μM, a linear increase in conductivity with hole concentration is observed suggesting that additional holes, above this threshold concentration, are mobile. Given the relationship between conductivity, σ, charge density, n, and mobility, μ, ($\sigma = ne\mu$) we obtain a value of $\mu_{AC} = 0.0154 \pm 0.00383$ cm^2/V·s from a straight line fit to the, above-threshold, linear region of σ vs n in Figure 2b. This mobility is the isotropic value (average over three dimensions) although we expect charge motion to mostly confined to lamellae, being fastest along the chain (crystallographic c axis) or in the π- π stacking direction (b axis), along the long axis of the nanowire; conductive AFM studies[19a, 22b] have shown the transport along the a axis to be three to four orders of magnitude slower.

These microwave conductivity measurements show very different behavior than those of Liu and Chen.[16] We see *no initial rise in conductivity* with doping followed by an increase, whereas they saw the largest increases in conductivity at the lowest doping levels. The lack of

an increase in conductivity with hole concentration in the 0 – 5 μM region in Figure 2 is suggestive of a dissociation constant for ion pairs that is < 10^{-6} so that the vast majority of ions would be paired in this concentration range.

The increase in conductivity at higher doping levels is similar to observations in doped organic semiconductor films, where at low doping levels, the ionized dopants present deep traps to the charges but at high doping levels, the average spacing between counterions decreases, allowing their potential wells to overlap, and their barrier heights to be reduced.[10a] We hypothesize that if the F_4TCNQ anions remain outside the aggregates, holes in the aggregate will tend to be drawn to the surface. Based on reported nanowire dimensions and lamellae spacing, we expect 3 lamellae along the crystallographic a axis.[19a, 30] At 5 μM, of P3HT holes, the aggregate is about one third full based on our estimates above for L_p. As these surface states get filled, subsequent holes would be forced to occupy the central lamella and experience a reduced coulomb attraction to counterions. This could explain why we observe a turn on in conductivity and why we obtain a mobility that is similar to that reported for free holes in P3HT.[17] A more general explanation would simply be that the holes fill up immobile "trap" states initially, but as the density of states is filled, states that enable higher mobility become occupied.

We might expect the conductivity to start to decrease again when the charges completely fill the aggregates and block each other. Our data in Figure 2b may indicate the start of this process, where our calculated concentration of ions gives 1 hole/10 PRU which is approaching our estimate of the polaron length of 8 PRU. Investigating this possibility further would require a stronger electron acceptor as the equilibrium for charge transfer from F_4TCNQ limits the concentration of holes that can be created on the aggregates.

To investigate the hypothesis that F_4TCNQ anions might be predominantly around the outer surface of the aggregates, we repeated the experiment on a fresh nw-P3HT solution but intentionally tried to intercalate the F4TCNQ anions into the aggregate. As a control, in the first

step, the aggregates were doped with F_4TCNQ after they had been created. As shown in SI Figure S7b, we recorded a change in conductivity consistent with the data in Figure 2b. We then heated up the solution to dissolve the aggregates and reverse the doping process. The solution was then cooled at 5 ºC for 6 days to reform the aggregates and the absorption shows the same concentration of ions were recreated (Figure S7a). This time, the conductivity was 4 times smaller despite being the same solution with the same concentration of ions. We speculate that by forming the aggregates in the presence of F_4TCNQ, there is a chance for more F_4TCNQ anions to be intercalated inside, which could lower the ability for P3HT holes to escape their counterion, and also cause a disruption to transport along the nanowire. Support for this concept comes from Doung *et al*. who investigated P3HT/F_4TCNQ films spun cast from chlorobenzene by grazing incidence X-ray diffraction, and observed a new crystal phase emerge above a certain mole fraction of dopant.[9] This new crystal phase has been attributed to intercalation of F_4TNCQ molecules into the crystalline region of P3HT. Moulé and coworkers also found a greater change in conductivity with ionized dopant concentration for sequentially processed films, where the P3HT films retained the lattice parameters of the neutral films.[27] The exact degree to which the dopants penetrate the aggregates, and the aggregate crystal structure will depend on the solvent, temperature and when the dopant is added.[27, 31] While we cannot determine the exact degree of dopant penetration into the aggregates, our results suggest that there is more penetration into the aggregates when the aggregates form in the presence of dopant rather than when the dopant is added after their formation.

To test our interpretation of the microwave conductivity data, DC conductivity was used to determine the dissociation constant of the ion pairs. The results of one of these experiments, in which F_4TCNQ was added to ~ 30 mL of nw-P3HT in toluene, is shown in **Figure 3a**. A sharp increase in conductivity is observed upon increasing ion concentration for low doping levels. This increase in conductivity levels off, before decreasing at higher ion concentrations. Without knowing the exact limiting molar conductivity of the species involved, we estimate a

range of 20 – 50 Scm^2/mole for F_4TCNQ anions based on measurements of electrolyte ions in solvents of similar viscosity;[18] the aggregate molar conductivity is assumed to be negligible. The maximum conductivity values of ~ 500 pS/cm would correspond to a free ion concentration of 10 – 25 nM confirming that essentially all ions remain paired at the concentrations studied in Figure 2. Ranges for the predicted conductivity from simple ion pairs using standard dissociation models[11] give an indication that the dissociation constant could be > 10^{-9}.

Given that we would not expect dissociation of ions from aggregates to follow traditional ion pairing models we developed a simple electrostatic model in SI for the *j*th dissociation constant for the *j*th F_4TCNQ anion to escape the increasingly charged aggregate. Since the conductivity function depends strongly on the number of charges per aggregate, we performed the DC conductivity experiment on two solutions that started with different concentrations of neutral nw-P3HT, created from the same stock solution. The conductivity is shown in Figure 3b. Despite the simplicity of the model, it describes the observations of conductivity that rises and then remains constant due to the increasing difficulty for F_4TCNQ anions to leave an aggregate as it develops an increasingly net-positive charge. A global fit to data shown in Figure 3b gave the initial dissociation for the first ion to be between 5.31×10^{-9} and 1.50×10^{-8} for estimated molar conductivities of 50 and 20 Scm^2/mole respectively.

We can now estimate the overall standard free energy to go from a neutral aggregate and F_4TCNQ to separated ions, ΔG°_{fi}, as shown in Figure 3c. Since we calculated the electron transfer equilibrium constant in terms of repeat units, this total free energy more accurately describes the process occurring with a small chunk of aggregate with only one site for the charge to reside (i.e. L_p repeat units). From $\Delta G^{\circ}_{fi} = -RTln(K^{\circ}_{et}K^{\circ}_{d})$, we find the free ions to be higher in energy than neutral state by 0.27 ± 0.05 eV. We qualify this by noting that the neutral states may have some degree of stabilization through charge transfer complex formation with the solvent or s-P3HT. Despite this, we are surprised at the massive disparity between our

experimentally determined value and what would be predicted based on reported HOMO LUMO levels[23] which suggest the process would be exoergic by 0.6 eV.

In summary, by selectively doping P3HT aggregates in non-polar solvents with F_4TCNQ, we have measured the energetics of electron transfer and charge dissociation in a model system relevant to charge escape in molecular films. We estimate a remarkably large dissociation constant in toluene between F_4TCNQ anions and delocalized holes on the P3HT aggregates of 10^{-8} on the molar scale. We do not find evidence from either DC conductivity or microwave conductivity that supports reports of free ions at micromolar concentrations following doping of P3HT in benzene. However, we hypothesize that such a result may be possible with an electron acceptor that is more delocalized than F_4TCNQ or in a more polar medium. The product of the electron transfer and dissociation equilibrium constants suggests that in non-polar media, the F_4TCNQ LUMO is actually about 0.27 eV higher in energy than the nw-P3HT HOMO rather than 0.6 eV below as reports suggest. This discrepancy of nearly one electron volt indicates the need for improved methods to determine and reference redox potentials accurately in non-polar environments, particularly when it comes to comparing oxidation and reduction potentials.

Experimental Section

Materials: Regioregular poly(3-hexylthiophene-2,5-diyl) (72 kD, Pd = 2.5, Reg 91%) was purchased from Rieke Metals and used as received. 2,3,5,6-tetrafluoro-7,7,8,8-tetracyanoquinonedimethane was purchased from Sigma-Aldrich and used as received. Toluene and o-xylene were purchased Aldrich and dried over 5 Å molecular sieves. All solutions were prepared in an argon atmosphere glovebox.

Fabrication of P3HT Nanofibers: In a glass centrifuge tube, toluene (5 mL) was added to RR-P3HT (40 mg). The suspension was sonicated for approximately 10 minutes, then heated to 80 ºC in a mineral oil bath, at which point the solution became a bright orange color,

indicative of solvated P3HT. The temperature of the mineral oil bath was decreased at a rate of 20 ºC/min to RT, where it was held for 5 days. Over this 5-day period, the solutions went from bright orange to dark brown/purple. The resulting suspensions were centrifuged at 4650 rpm at -9 ºC for 3 hours and the supernatant was decanted approximately 5 times, until the supernatant no longer appeared orange in color. The resulting purple solid was kept as a concentrated suspension and diluted upon use.

Microwave Conductivity Measurements: Microwave conductivity measurements were performed on an in-house instrument, built in collaboration with the National Renewable Energy Laboratory. Microwave power from a Hittite HMC-T2240 source is coupled to X-band rectangular waveguide with a waveguide-to-coax adapter. An end section of WR-90 waveguide, sealed with a polytetrafluoroethylene window with a copper iris formed a 2.54 cm long cavity that was filled with sample solution. A Schottky diode detector measures a voltage signal of the reflected microwaves which is digitized using a WaveJet 314A oscilloscope. A cross coupler (30 dB) is placed between the source and sample cavity and is used divert a small amount of microwave power from the system to be measured to account for changes in microwave source power output between measurements of individual samples. The voltage signals are converted to power by a calibration of the power-voltage response of the detectors. Incident microwave power was measured by replacing the sample cavity with a copper plate, which represents total reflection of the microwaves.

DC Conductivity measurements: DC conductivity of solutions was measured at room temperature in an argon glovebox with a Scientifica Model 627 Conductivity Meter. Solution volumes were typically 30 mL. The solution was stirred briefly between each addition of dopant.

UV/Vis/NIR absorptions spectroscopy: UV/Vis/NIR Absorption spectra were acquired in 1 cm or 2 mm path length cells on either an Agilent Cary 60 UV/Vis spectrometer, Agilent Cary

5000 UV/vis/NIR spectrometer, or an Ocean Optics USB2000+ spectrometer with a Xe arc lamp source (Photon Technologies International).

Acknowledgements
This material is supported by the U.S. Department of Energy, Office of Science, Office of Basic Energy Sciences, Division of Chemical Sciences, Geosciences & Biosciences under Contract DE-SC0012704. This project was also supported in part by the U.S. Department of Energy, Office of Science, Office of Workforce Development for Teachers and Scientists (WDTS) under the Science Undergraduate Laboratory Internships Program (SULI) and in part by the Brookhaven National Laboratory (BNL), Chemistry Division under the BNL Supplemental Undergraduate Research Program (SURP). The authors wish to thank J. R. Miller for useful discussions.

References

[1] a) Z. Xiao, X. Jia, L. Ding, *Sci. Bull.* **2017**, *62*, 1562; b) L. Meng, Y. Zhang, X. Wan, C. Li, X. Zhang, Y. Wang, X. Ke, Z. Xiao, L. Ding, R. Xia, H.-L. Yip, Y. Cao, Y. Chen, *Science* **2018**, *361*, 1094.

[2] a) C. K. Chiang, C. R. Fincher, Y. W. Park, A. J. Heeger, H. Shirakawa, E. J. Louis, S. C. Gau, A. G. MacDiarmid, *Phys. Rev. Lett.* **1977**, *39*, 1098; b) N. Basescu, Z. X. Liu, D. Moses, A. J. Heeger, H. Naarmann, N. Theophilou, *Nature* **1987**, *327*, 403; c) A. J. Heeger, S. Kivelson, J. R. Schrieffer, W. P. Su, *Rev. Mod. Phys* **1988**, *60*, 781.

[3] N. A. Pace, O. G. Reid, G. Rumbles, *ACS Energy Lett.* **2018**, *3*, 735.

[4] a) S. Gélinas, A. Rao, A. Kumar, S. L. Smith, A. W. Chin, J. Clark, T. S. van der Poll, G. C. Bazan, R. H. Friend, *Science* **2014**, *343*, 512; b) F. Provencher, N. Bérubé, A. W. Parker, G. M. Greetham, M. Towrie, C. Hellmann, M. Côté, N. Stingelin, C. Silva, S. C. Hayes, *Nat. Commun.* **2014**, *5*, 4288.

[5] T. M. Burke, S. Sweetnam, K. Vandewal, M. D. McGehee, *Adv. Energy Mater.* **2015**, *5*, 1500123.

[6] S. Barth, D. Hertel, Y. H. Tak, H. Bässler, H. H. Hörhold, *Chem. Phys. Lett.* **1997**, *274*, 165.

[7] S. N. Hood, I. Kassal, *J. Phys. Chem. Lett.* **2016**, *7*, 4495.
[8] a) T. M. Burke, M. D. McGehee, *Adv. Mater.* **2014**, *26*, 1923; b) C. Groves, *Energy Environ. Sci.* **2013**, *6*, 1546.
[9] D. T. Duong, C. Wang, E. Antono, M. F. Toney, A. Salleo, *Org. Electron.* **2013**, *14*, 1330.
[10] a) V. I. Arkhipov, E. V. Emelianova, P. Heremans, H. Bässler, *Phys. Rev. B* **2005**, *72*, 235202; b) G. Zuo, H. Abdalla, M. Kemerink, *Phys. Rev. B* **2016**, *93*, 235203.
[11] Y. Marcus, G. Hefter, *Chem. Rev.* **2006**, *106*, 4585.
[12] G. Dicker, M. P. de Haas, L. D. A. Siebbeles, J. M. Warman, *Phys. Rev. B* **2004**, *70*, 045203.
[13] a) M. P. De Haas, J. M. Warman, *Chem. Phys.* **1982**, *73*, 35; b) O. Reid, G., D. Moore, T., Z. Li, D. Zhao, Y. Yan, K. Zhu, G. Rumbles, *J. Phys. D: Appl. Phys.* **2017**, *50*, 493002; c) A. Saeki, S. Seki, T. Sunagawa, K. Ushida, S. Tagawa, *Philos. Mag.* **2006**, *86*, 1261.
[14] a) M. J. Bird, O. G. Reid, A. R. Cook, S. Asaoka, Y. Shibano, H. Imahori, G. Rumbles, J. R. Miller, *J. Phys. Chem. C* **2014**, *118*, 6100; b) J. M. Warman, A. M. Van De Craats, *Mol. Cryst. Liq. Cryst.* **2003**, *396*, 41.
[15] a) T. J. Savenije, A. J. Ferguson, N. Kopidakis, G. Rumbles, *J. Phys. Chem. C* **2013**, *117*, 24085; b) D. H. K. Murthy, M. Gao, M. J. W. Vermeulen, L. D. A. Siebbeles, T. J. Savenije, *J. Phys. Chem. C* **2012**, *116*, 9214.
[16] C.-Y. Liu, S.-A. Chen, *J. Chem. Phys.* **2009**, *130*, 204906.
[17] G. Dicker, M. P. de Haas, J. M. Warman, D. M. de Leeuw, L. D. A. Siebbeles, *J. Phys. Chem. B* **2004**, *108*, 17818.
[18] R. J. LeSuer, C. Buttolph, W. E. Geiger, *Anal. Chem.* **2004**, *76*, 6395.
[19] a) J. D. Roehling, I. Arslan, A. J. Moule, *J. Mater. Chem.* **2012**, *22*, 2498; b) E. T. Niles, J. D. Roehling, H. Yamagata, A. J. Wise, F. C. Spano, A. J. Moulé, J. K. Grey, *J. Phys. Chem. Lett.* **2012**, *3*, 259.
[20] F. C. Spano, *Acc. Chem. Res.* **2010**, *43*, 429.
[21] a) J. Gao, E. T. Niles, J. K. Grey, *J. Phys. Chem. Lett.* **2013**, *4*, 2953; b) W. C. Tsoi, S. J. Spencer, L. Yang, A. M. Ballantyne, P. G. Nicholson, A. Turnbull, A. G. Shard, C. E. Murphy, D. D. C. Bradley, J. Nelson, J.-S. Kim, *Macromolecules* **2011**, *44*, 2944.
[22] a) F. M. McFarland, L. R. Bonnette, E. A. Acres, S. Guo, *J. Mater. Chem. C* **2017**, *5*, 5764; b) F. M. McFarland, C. M. Ellis, S. Guo, *J. Phys. Chem. C* **2017**, *121*, 4740.
[23] K. Tang, F. M. McFarland, S. Travis, J. Lim, J. D. Azoulay, S. Guo, *Chem. Commun.* **2018**, *54*, 11925.
[24] a) W. Gao, A. Kahn, *Appl. Phys. Lett.* **2001**, *79*, 4040; b) H. Méndez, G. Heimel, S. Winkler, J. Frisch, A. Opitz, K. Sauer, B. Wegner, M. Oehzelt, C. Röthel, S. Duhm, D. Többens, N. Koch, I. Salzmann, *Nat. Commun.* **2015**, *6*, 8560.
[25] L. Müller, D. Nanova, T. Glaser, S. Beck, A. Pucci, A. K. Kast, R. R. Schröder, E. Mankel, P. Pingel, D. Neher, W. Kowalsky, R. Lovrincic, *Chem. Mater.* **2016**, *28*, 4432.
[26] P. Pingel, D. Neher, *Phys. Rev. B* **2013**, *87*, 115209.
[27] I. E. Jacobs, E. W. Aasen, J. L. Oliveira, T. N. Fonseca, J. D. Roehling, J. Li, G. Zhang, M. P. Augustine, M. Mascal, A. J. Moule, *J. Mater. Chem. C* **2016**, *4*, 3454.
[28] J. M. Schins, P. Prins, F. C. Grozema, R. D. Abellón, M. P. d. Haas, L. D. A. Siebbeles, *Rev. Sci. Instrum.* **2005**, *76*, 084703.
[29] P. P. Infelta, M. P. de Haas, J. M. Warman, *Radiat. Phys. Chem.* **1977**, *10*, 353.
[30] N. E. Persson, P.-H. Chu, M. McBride, M. Grover, E. Reichmanis, *Acc. Chem. Res.* **2017**, *50*, 932.
[31] I. E. Jacobs, C. Cendra, T. F. Harrelson, Z. I. Bedolla Valdez, R. Faller, A. Salleo, A. J. Moulé, *Materials Horizons* **2018**, *5*, 655.

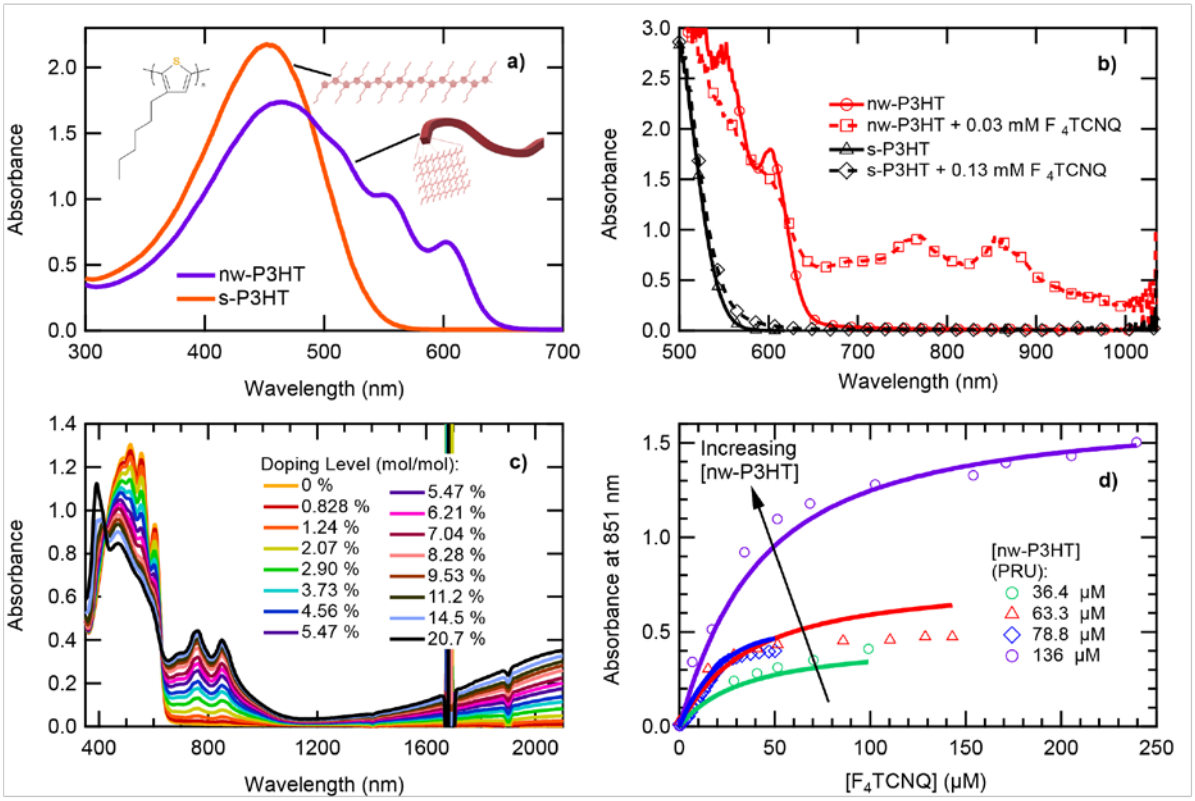

Figure 1. a) Absorption spectra of 1.58 mM (PRU) RR-P3HT in toluene in a 2 mm pathlength cell, both as a mixture of nanowires and solubilized chains (purple) and following heating to solubilize all the chains (orange). b) Spectra showing the doping of nw-P3HT with F_4TCNQ in toluene to make ions, and the absence of ions when F_4TCNQ is added to s-P3HT c) Spectra obtained upon doping a nw-P3HT solution with F_4TCNQ in toluene with a path length of 1 cm. The initial nw-P3HT concentration was 0.0788 mM (PRU), reducing to 0.0630 mM by the last addition of the 0.251 mM F_4TCNQ solution. d) The absorbance at 851 nm as a function of F_4TCNQ concentration from four separate experiments including the one shown in c), normalized to a path length of 1 cm. Solid lines show the results of a global fit using equation 1 which finds an equilibrium constant of K_{eq} = 3750 and polaron length of 8.41 PRU.

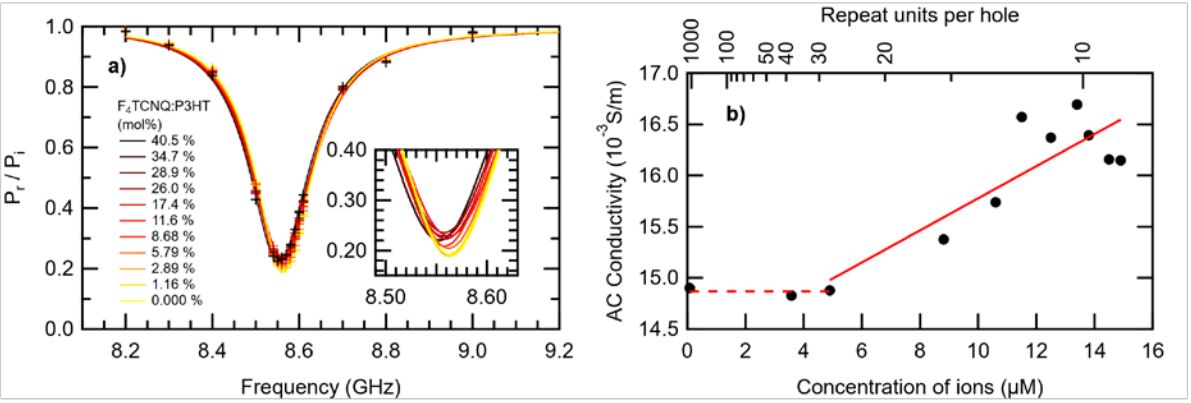

Figure 2: a) Plot showing the fraction of power reflected from the waveguide cavity versus microwave frequency (points) with fits (solid lines) using the waveguide impedance model described in the text. The cavity contains a 0.136 mM (PRU) solution of nw-P3HT in toluene with various amounts of F_4TCNQ added. b) The conductivity of the solutions from a) plotted as a function of ion concentration observed from optical absorption measurements. The slope of the linear region corresponds to a mobility of 0.015 ± 0.004 $cm^2V^{-1}s^{-1}$.

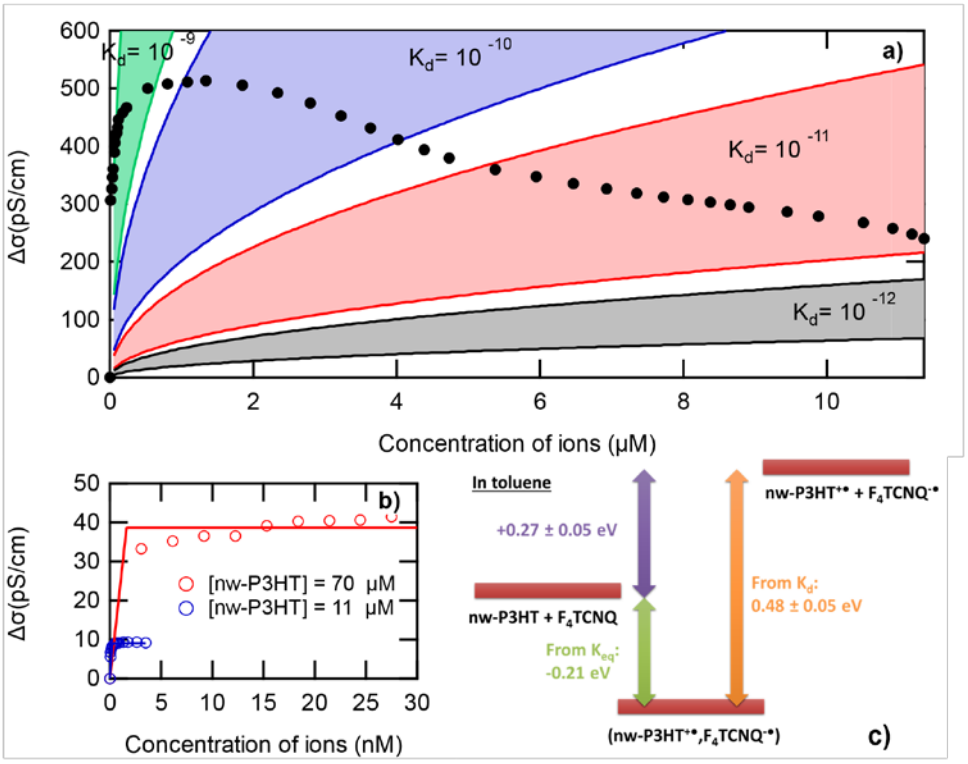

Figure 3. a) DC conductivity from a solution containing 137 μM (PRU) nw-P3HT with various amounts of F_4TCNQ in toluene. Shaded areas contain bounds for conductivity from equations used by LeSuer[18] for various dissociation constants, with upper limit having limiting molar conductivity, $\Lambda^{\circ} = 50$ Scm^2mole^{-1} and lower limit having 20 Scm^2mole^{-1}. b) DC conductivity from solutions containing 70 μM (PRU) and 11 μM (PRU) nw-P3HT. Solid lines show the result of a global fit with $\Lambda^{\circ} = 50$ Scm^2mole^{-1} which gave $K_d = 5.31 \times 10^{-9}$ ($\Delta G_d = 0.490$ eV) for and L = 1.49 microns. c) Standard free energy diagram summarizing the results from the optical absorption experiments in Figure 1, and the DC conductivity.

Supporting Information

Energetics and escape of interchain-delocalized ion pairs in non-polar media

John H. Burke, and Matthew J. Bird*

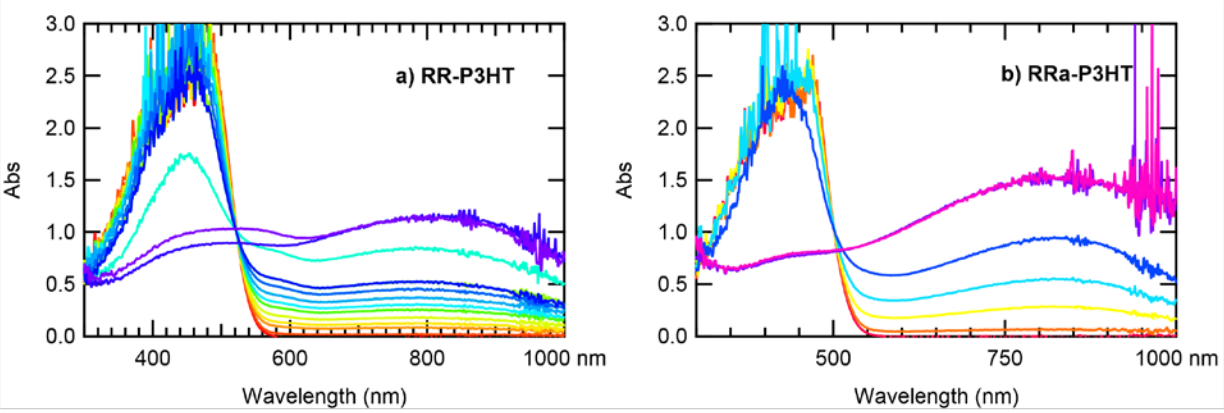

Figure S1. Stirring a speck of $NOPF_6$ in solutions of a) RR-P3HT 0.633 mM (PRU) and b) RRa-P3HT 0.683 mM to make P3HT holes and PF_6^- in benzene. Stirring time between traces is of the order of minutes. The similarities in shape around 600 nm between the traces in a) and spectra reported by Liu[1] suggest that RR P3HT was used in the latter case also.

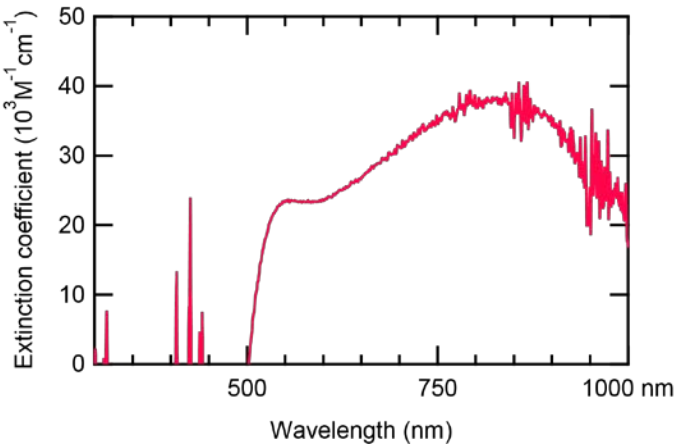

Figure S2. Spectrum of RRa P3HT cation in benzene obtained by a difference between two traces in Figure S1b, scaled to the extinction coefficient determined by dedoping the aggregates with a TMPD solution.

Determination of nw-P3HT Concentration

The relative intensities of the vibrionic transitions of nw-P3HT are sensitive to the degree of intra- and interchain coupling[2] which can vary due to processing conditions.[3] Thus, extinction

coefficients determined for aggregates may not match those produced under different conditions. Therefore, to quantify the concentration of nw-P3HT in solution, we decompose spectra into the spectrum of the solvated polymer, and 4 Gaussian functions to reproduce the spectrum of the aggregates. We allow the relative intensities of the Gaussians to vary and make the assumption that the area under the sum of the Gaussians is proportional to the concentration of the aggregates. The area under the absorption spectrum (in eV) for a 1 M solution of nw-P3HT in a 1 cm path length cell is determined to be 7147.3, based upon a global fit to a series of solutions containing s-P3HT and nw-P3HT. Properties of the Gaussians used are shown in Table S1

Table S1.

$E_{0\text{-}0}$ (eV)	$W_{0\text{-}0}$ (eV)	$E_{0\text{-}1}$ (eV)	$W_{0\text{-}1}$ (eV)	$E_{0\text{-}2}$ (eV)	$W_{0\text{-}2}$ (eV)	$E_{0\text{-}3}$ (eV)	$W_{0\text{-}3}$ (eV)
2.049	0.0575	2.218	0.0695	2.373	0.0772	2.517	0.0976

Additional evidence for the lack of doping of s-P3HT

When adding F_4TCNQ to a solution of RR-P3HT that had almost all of the chains solubilized, it was observed that due to the small amount of nw-P3HT present, some ions were formed and an associated bleach of the neutral aggregate peak at ~600 nm was observed. Once the peak was completely bleached, there was no further increase in absorption from ions as noted in Figure S3b which tracks the absorption at 852 nm. Presumably, additional ions would form at later times as more chains aggregate on a slower timescale.[4]

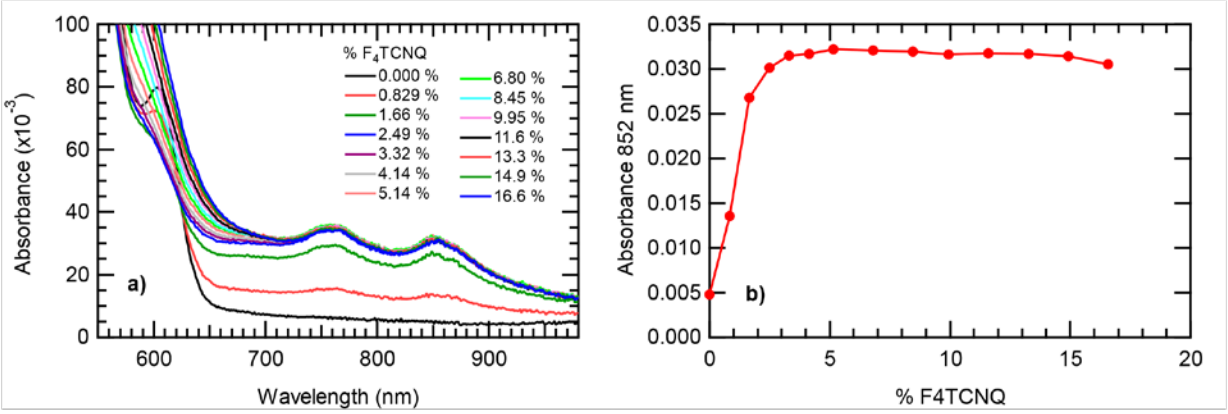

Figure S3. a) Spectral evolution upon addition of F_4TCNQ to a solution of 37 µM (PRU) RR-P3HT in o-xylene. b) Evolution of absorbance at 852 nm from the traces in Figure S3a.
Adding F_4TCNQ to RRa-P3HT showed no sign of ions as shown in Figure S4.

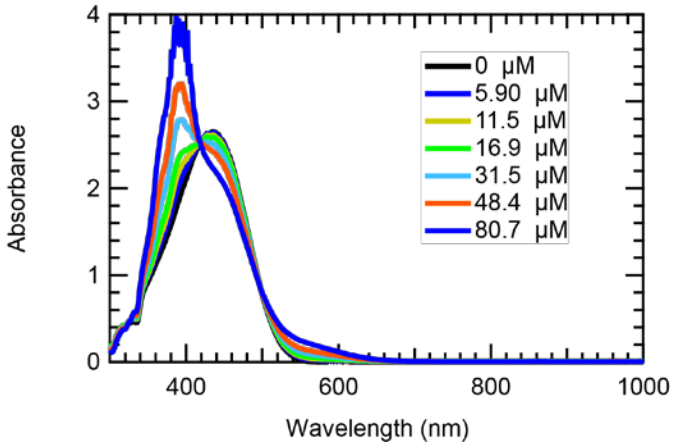

Figure S4. Various additions of F_4TCNQ to a solution of RRa-P3HT in 34 µM (PRU) in o-xylene.

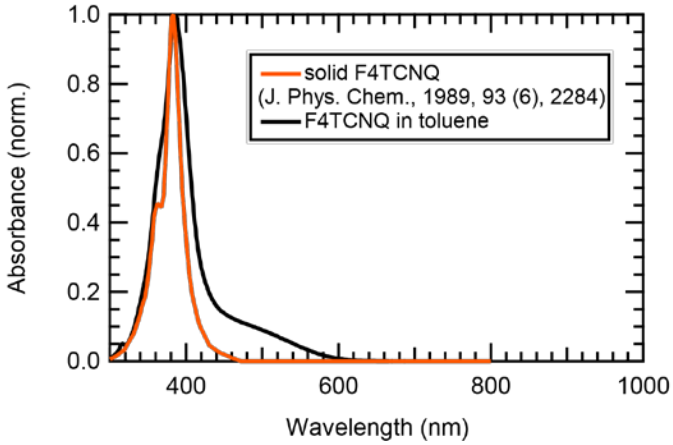

Figure S5. Spectra of solid F_4TCNQ from and F_4TCNQ dissolved in toluene showing that the spectral features above 500 nm in figures S3 and S4 may be from F_4TCNQ complexed with the solvent. Reprinted with permission from ref.[5] Copyright 1989 American Chemical Society.

Global Fitting to UV/Vis/NIR Absorption Data

Charge transfer between F_4TCNQ and nw-P3HT was modeled as neutral donor and acceptor species forming an ion pair. The fitting equation, derived from the equilibrium constant expression, is shown in Equation 1. The relevant donor concentration is the nw-P3HT concentration in PRU, which was determined by decomposing the neutral P3HT spectrum to a sum of the spectrum of solvated chains and 4 gaussians to represent the vibrionic transitions of the nw‘s, as described above. The blue trace in Figure 1d was fit to a slightly modified equation due to the polymer concentration not being held constant during the addition of F_4TCNQ: the donor concentration C_D was replaced by $C_{Do}*(1 - C_A/C_{Ao})$. Because the nw-P3HT concentrations given are the polymer repeat unit (PRU) concentration, the polaron length, L_p, is introduced as a parameter and represents the number of neutral repeat units consumed upon hole transfer to the nanowire.

$$D + A \rightleftharpoons (D^+, A^-) \qquad \text{Scheme S1}$$

$$\mathrm{K_{eq}} = \frac{[(\mathrm{D}^+, \mathrm{A}^-)]}{[\mathrm{D}][\mathrm{A}]} = \frac{A/\varepsilon b}{(C_D - L_p \frac{A}{\varepsilon b})(C_A - \frac{A}{\varepsilon b})} \quad \text{(S1)}$$

$$A = \varepsilon b \left(\frac{K_{eq}C_D + K_{eq}L_pC_A + 1 - \sqrt{\left(K_{eq}C_D + K_{eq}L_pC_A + 1\right)^2 - 4L_pK_{eq}^2C_DC_A}}{2L_pK_{eq}} \right) \quad \text{(S2)}$$

$$A = \varepsilon b \left(\frac{K_{eq}C_{D_0}\left(1 - \frac{C_A}{C_{A_0}}\right) + K_{eq}L_pC_A + 1 - \sqrt{\left(K_{eq}C_{D_0}\left(1 - \frac{C_A}{C_{A_0}}\right) + K_{eq}L_pC_A + 1\right)^2 - 4L_pK_{eq}^2C_{D_0}\left(1 - \frac{C_A}{C_{A_0}}\right)C_A}}{2L_pK_{eq}} \right) \quad \text{(S3)}$$

Stability of nw-P3HT holes created by F$_4$TCNQ doping

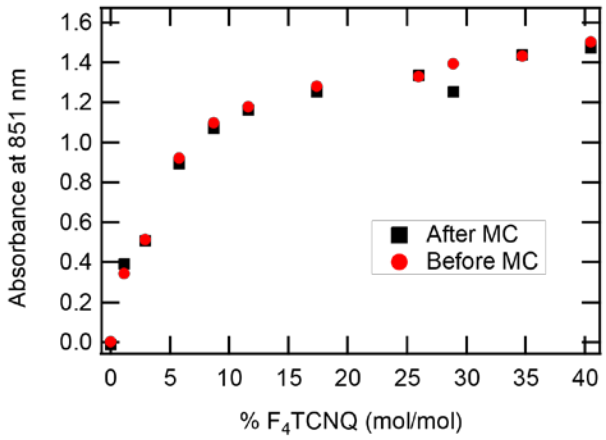

Figure S6. Optical absorption at 851 nm from solutions before and after microwave conductivity measurements were performed demonstrating the stability of ions over the time scale of the experiment.

Ion intercalation

We investigated the effects of ion intercalation on the microwave conductivity of p-doped nw-P3HT. Microwave conductivity measurements were performed on nw-P3HT/F$_4$TCNQ solutions in toluene. The solutions were then heated to disassemble the nw's and dedope the polymer, then cooled at 5 ºC for 6 days to reform the nw's with the dopant present, under the assumption that the nw's formed under these conditions would show increased counterion intercalation, a process that has been employed to assign changes in lattice parameters upon doping P3HT films.[6] Figure S7b shows that the microwave conductivity was reduced by a factor of ~4 upon heating and cooling, showing that the different processing conditions do have an effect. If

this effect is attributable to increased ion intercalation, it would suggest that the mobility of holes or fraction of untrapped holes is greater for nw-P3HT without intercalated counterions. This can be rationalized by a greater charge separation when the counterions are not intercalated into the aggregates.

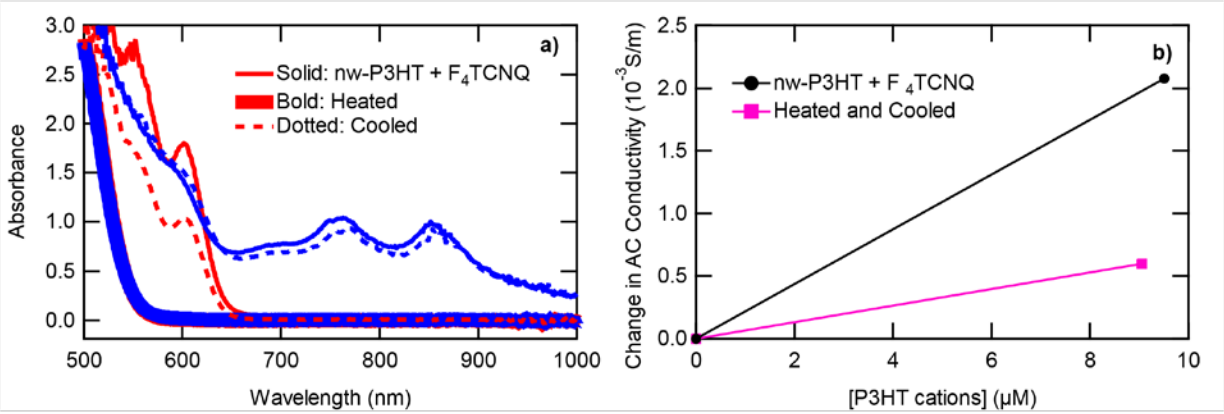

Figure S7. a) Absorption spectra of nw-P3HT solutions in toluene with 0 mM (red) and 0.03 mM (blue) F_4TCNQ. Spectra of as-prepared (solid traces), heated (bold), and cooled (dotted) solutions are shown. Microwave conductivity as a function of charge concentration for solutions of nw-P3HT that were doped after aggregate formation (black points) and then heated to disassemble the aggregates and dedope the polymer, then cooled to form aggregates in the presence of F_4TCNQ (pink squares).

Derivation of conductivity model for aggregates

Here we present a simple model to explain the key principles behind the dissociation of F_4TCNQ anions from their counterions, which are holes on P3HT aggregates. We seek an expression for the equilbrium variation of *free* (unpaired) F_4TCNQ ion concentration, which contributes to DC conductivity, with total concentration of ions (paired and unpaired). Ion pairing is easily described in the case of single ion pairs such as in an electrolyte, but the confinement of multiple charges on one object changes the functional dependence.

For simplicity we assume that all aggregates are the same length and have the same number of holes, we can write the total concentration of ions, c_i, as the concentration of all aggregates, multiplied by number of holes per aggregate, β:

$$c_i = [Agg^{ALL}]\beta \tag{S4}$$

To obtain the concentration of F_4TCNQ anions that have escaped from their P3HT hole counterion, we consider the various net charges that aggregates (dressed with coulombically bound F_4TCNQ counterions) might have depending on how many F_4TCNQ anions have escaped. At all times each aggregate has β holes. If no F4TCNQ anions escape, there would be β F4TCNQ anions around the aggregate and we consider it to have a net charge of zero. If one F_4TCNQ anion escapes, our notation would give a net charge of +1 to the aggregate. The total concentration of *free* (F_4TCNQ) ions, c_{fi}, is given by the sum:

$$c_{fi} = [Agg^{+}] \times 1 + [Agg^{2+}] \times 2 + \cdots \left[Agg^{\beta+}\right] \times \beta \tag{S5}$$

$$c_{fi} = \sum_{i=1}^{\beta} \left[Agg^{i+}\right] \times i \tag{S6}$$

We are using a notation where Agg^{j+} is the object described by:

$$Agg^{j+} = \left(nwP3HT^{\beta+}, (\beta - j)F_4TCNQ^{-}\right) \tag{S7}$$

The total concentration of all ions is given by:

$$c_i = [Agg^{ALL}]\beta = \left([Agg^{0}] + [Agg^{+}] + [Agg^{2+}] + \cdots \left[Agg^{\beta+}\right]\right)\beta \tag{S8}$$

$$c_i = \beta \sum_{i=0}^{\beta} \left[Agg^{i+}\right] \tag{S9}$$

The dissociation constant for the first F_4TCNQ anion to:

$$K_1 = \frac{[Agg^{+}]c_{fi}}{[Agg^{0}]} \tag{S10}$$

$$K_2 = \frac{[Agg^{2+}]c_{fi}}{[Agg^{+}]} \tag{S11}$$

With general relationship:

$$K_i = \frac{\left[Agg^{i+}\right]c_{fi}}{[Agg^{(i-1)+}]} \tag{S12}$$

up to the final dissociation constant where $i = \beta$.

The equilibrium constants can be used to eliminate all the terms containing concentrations of positively charged aggregates using:

$$[Agg^{+}] = \frac{[Agg^{0}]K_1}{c_{fi}} \tag{S13}$$

$$[Agg^{2+}] = \frac{[Agg^{+}]K_2}{c_{fi}} = \frac{[Agg^{0}]K_1K_2}{{c_{fi}}^2} \tag{S14}$$

up to

$$\left[Agg^{\beta+}\right] = \frac{[Agg^{0}]K_1K_2 \dots K_\beta}{{c_{fi}}^\beta} \tag{S15}$$

So a final expression for the concentration of free ions, i.e. the F_4TCNQ^- anions that give rise to the conductivity is given by:

$$c_{fi} = \frac{[Agg^{0}]K_1}{c_{fi}} \times 1 + \frac{[Agg^{0}]K_1K_2}{{c_{fi}}^2} \times 2 + \cdots \frac{[Agg^{0}]K_1K_2 \dots K_\beta}{{c_{fi}}^\beta} \times \beta \tag{S16}$$

$$c_{fi} = [Agg^{0}] \sum_{i=1}^{\beta} \frac{\prod_{j=1}^{i} K_j}{{c_{fi}}^i} \times i \tag{S17}$$

Similarly, the concentration of all, free+paired, ions (that would be determined by an optical absorption experiment) is given by:

$$\begin{aligned} c_i &= [Agg^{ALL}]\beta \\ &= \left([Agg^{0}] + \frac{[Agg^{0}]K_1}{c_{fi}} + \frac{[Agg^{0}]K_1K_2}{{c_{fi}}^2} + \cdots \frac{[Agg^{0}]K_1K_2 \dots K_\beta}{{c_{fi}}^\beta}\right)\beta \end{aligned} \tag{S18}$$

$$c_i = \beta[Agg^{0}]\left(1 + \sum_{i=1}^{\beta} \frac{\prod_{j=1}^{i} K_j}{{c_{fi}}^i}\right) \tag{S19}$$

We can eliminate the remaining unknown parameter, $[Agg^{0}]$ to obtain:

$$c_i = \frac{\beta c_{fi}\left(1 + \sum_{i=1}^{\beta} \frac{\prod_{j=1}^{i} K_j}{{c_{fi}}^i}\right)}{\sum_{i=1}^{\beta} \frac{\prod_{j=1}^{i} K_j}{{c_{fi}}^i} \times i} \tag{S20}$$

Ideally, we want a function of $c_{fi}(c_i)$ which would be directly related to a plot of conductivity against concentration of all ions. We can achieve this by writing a function that finds the zero of the following equation:

$$0 = [Agg^{ALL}]\frac{\sum_{i=1}^{\beta}\frac{\prod_{j=1}^{i}K_j}{{c_{fi}}^i}\times i}{\left(1+\sum_{i=1}^{\beta}\frac{\prod_{j=1}^{i}K_j}{{c_{fi}}^i}\right)} - c_{fi} \tag{S21}$$

We can consider three cases in which we might estimate the dissociation constants.

Firstly, we could imagine infinitely long aggregates where the dissociation constant, K_j, for the *j*th F_4TCNQ to leave is the same as the first:

$$K_j = K_{j=1} \tag{S22}$$

In this special case we can solve the equation analytically using the fact that:

$$\frac{\sum_{i=1}^{N}a^i\times i}{(1+\sum_{i=1}^{N}a^i)} = \frac{\left(a(Na^{N+1}-Na^N-a^N+1)\right)}{(a-1)(a^{N+1}-1)} \tag{S23}$$

In the other extreme, we could imagine that the aggregate is infinitely compact, in which case we would expect the standard dissociation free energy, ΔG_d^0, to scale with the charge remaining on the aggregate giving $\Delta G_{d,j}^0 = j\Delta G_d^0$ for the *j*th dissocation energy. Since $K_d^0 = e^{-\frac{\Delta G_d^0}{k_B T}}$ we would expect the dissociation constant to vary according to:

$$K_j = \left(K_{j=1}\right)^j \tag{S24}$$

In the more general case, we considered how the dissociation constant might vary for subsequent dissociations using the model is Figure S8. In this very simple model, we assume the aggregate to be straight and the unpaired holes to distribute themselves with uniform spacing due to coulombic repulsion.

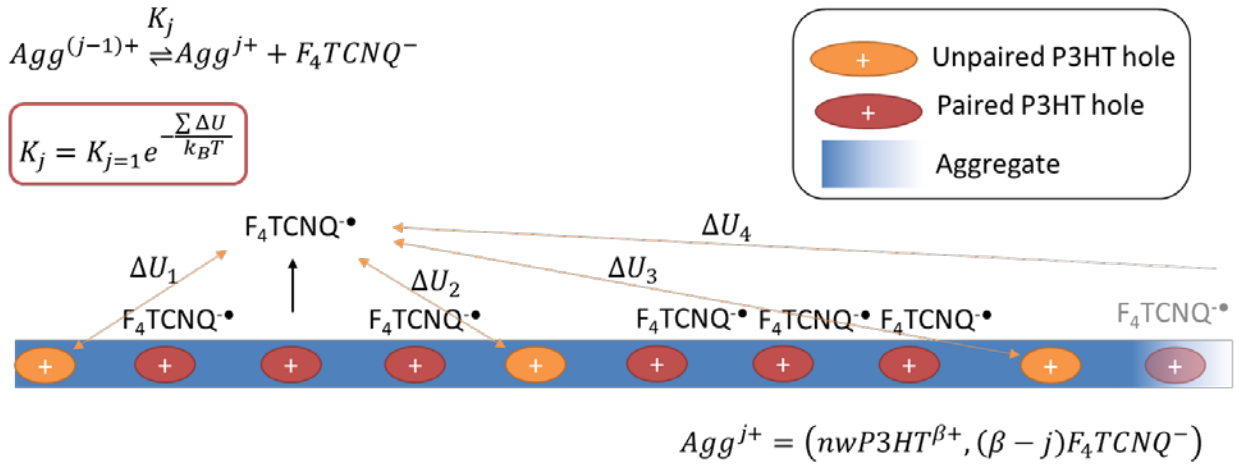

Figure S8. Simple model to estimate K_d values for subsequent dissociation constants.

A more sophisticated model would consider screening of distant aggregate charges by F_4TCNQ anions in the solvent, and account for the way the mobile charges on the aggregate would redistribute and average over probability distributions, however this simple model contains the core mechanism that would cause subsequent dissociations to become more difficult and recovers the limits for the dissociation constant behavior in long and short aggregates that are mentioned above.

Figure S9. shows a plot of the functional dependence of the *j*th dissociation constant on *j*. In this case, the initial dissociation constant was set to 10^{-8}.

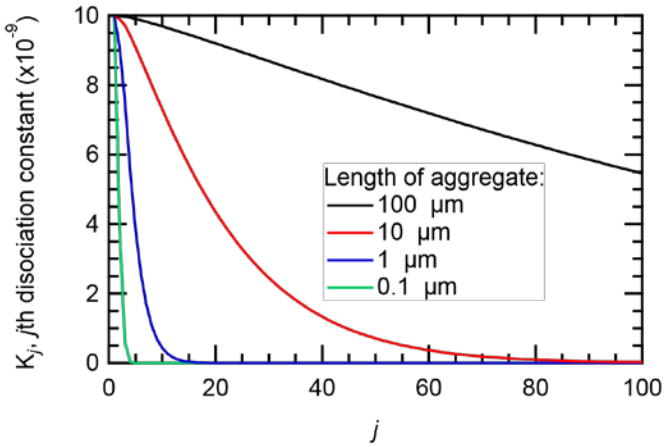

Figure S9. Dissociation constant for *j*th dissociation of an F_4TCNQ anion from P3HT aggregate which has a net charge of *j*-1. This is the equation shown in Figure S8 with the aggregate length set to 1 micron and the initial standard dissociation constant for the first F_4TCNQ anion to dissociate being 1×10^{-8} on the molar scale.

The results of fitting this function to the conductivity data in figure 3b are as follows:

For an estimated limiting molar conductivity of 20 Scm^2/mole, the best fit gave:

$K_d = 1.50 \times 10^{-8}$ ($\Delta G_d = 0.463$ eV) for and L = 4.80 microns

For an estimated limiting molar conductivity of 50 Scm^2/mole, the best fit gave:

$K_d = 5.31 \times 10^{-9}$ ($\Delta G_d = 0.490$ eV) for and L = 1.49 microns

We therefore estimate the standard free energy of dissociation to be 0.48 ± 0.05 eV. Relating this value to an initial separation between the ions using an equation for point charges is tempting although may have limited meaning; it would be 1.2 – 1.3 nm. The estimated lengths of the nanowires, L, which were completely free paramters are very reasonable.

References

[1] C.-Y. Liu, S.-A. Chen, *J. Chem. Phys.* **2009**, *130*, 204906.

[2] F. C. Spano, *Acc. Chem. Res.* **2010**, *43*, 429.

[3] a) E. T. Niles, J. D. Roehling, H. Yamagata, A. J. Wise, F. C. Spano, A. J. Moulé, J. K. Grey, *J. Phys. Chem. Lett.* **2012**, *3*, 259; b) J. D. Roehling, I. Arslan, A. J. Moule, *J. Mater. Chem.* **2012**, *22*, 2498.

[4] F. M. McFarland, L. R. Bonnette, E. A. Acres, S. Guo, *J. Mater. Chem. C* **2017**, *5*, 5764.

[5] D. A. Dixon, J. C. Calabrese, J. S. Miller, *J. Phys. Chem.* **1989**, *93*, 2284.

[6] a) D. T. Duong, C. Wang, E. Antono, M. F. Toney, A. Salleo, *Org. Electron.* **2013**, *14*, 1330; b) I. E. Jacobs, E. W. Aasen, J. L. Oliveira, T. N. Fonseca, J. D. Roehling, J. Li, G. Zhang, M. P. Augustine, M. Mascal, A. J. Moule, *J. Mater. Chem. C* **2016**, *4*, 3454.